**Preprints of the 19th World Congress**
**The International Federation of Automatic Control**
**Cape Town, South Africa. August 24-29, 2014**

# Comparative study of two global affine Linear Periodic Parameter Varying State Space model estimation algorithms

**J. Goos** * **R. Pintelon** *

* *Dept. ELEC, Fundamental Electricity and Instrumentation*
*Vrije Universiteit Brussel*
*Pleinlaan 2, 1050 Brussels, Belgium*
jan.goos@vub.ac.be

Abstract A comparative study is made between two global Linear Periodic Parameter-Varying (LPPV) identification algorithms. The first method is a state-of-the-art subspace identification method in the time domain. The second is a newly developed frequency domain approach, where the identification experiment is designed carefully so we can exploit the resulting structure. For both methods, the result is a state space model with an affine dependence on the varying parameters, which can be used for LPV control synthesis. Simulations show that the frequency domain procedure has a lower variance for identical experimental conditions.

## 1. INTRODUCTION

Although most physical systems are non-linear with respect to the input, they are usually modeled by a Linear Time-Invariant (LTI) representation as in Ljung [1999]. This model is a linearization of the nonlinear dynamics at a chosen operating point. In practical applications like the chemical industry, it is quite common to use the same plant for manufacturing different products, each with its own operational mode. In De Caigny [2009] a meta-model interpolates between local LTI descriptions to obtain a global model for all operating points. This intuitive approach is known as gain scheduling, and it requires the scheduling parameter to vary slowly, so the local static estimations remain approximately valid. Contrary to this local approach we will identify a Linear Parameter-Varying (LPV) plant, where the dynamics depend on some external scheduling parameters, as discussed in Rugh and Shamma [2000]. Only a single experiment is required, where both the scheduling and the input are varied.
Beside the local and global classification, there is also a model choice between an Input-Output (IO) form like in like Louarroudi et al. [2012], Lataire and Pintelon [2011] or a State Space (SS) representation as in Hench [1995]. From Tóth [2010] and Tóth et al. [2012], it is known that a conversion from one LPV model class to another is not as straightforward as in the LTI case.

There are some controller synthesis tools available for LPV systems, see, for example Lee and Park [2007] and Petersson and Löfberg [2011], but the models are commonly required to be transformed into state space form. We will therefore concentrate immediately on the LPV SS class, because it can be used directly in control design applications.

The aim of this paper is to compare two state-of-the-art LPV SS identification methods. We start by presenting the main ideas of both techniques. Section 2 discusses the time domain LPV subspace identification scheme of Felici et al. [2007], called periodic-MOESP, while Section 3 treats our newly developed frequency domain approach. The advantages and disadvantages of both methodologies are discussed in Section 4. Finally, in Section 5, we compare both methods on a simulation example. We summarize the results in Section 6.

### *1.1 Notation*

The Linear Parameter-Varying State Space equations are given in discrete time by

$$x_{(t+1)} = A\big(p_{(t)}\big)x_{(t)} + B\big(p_{(t)}\big)u_{(t)} \tag{1}$$

$$y_{(t)} = C\big(p_{(t)}\big)x_{(t)} + D\big(p_{(t)}\big)u_{(t)} \tag{2}$$

where $t$ is the discrete time step, going from 1 to the number of measurements $N$. We denote the number of inputs $u$, states $x$, outputs $y$ and scheduling variables $p$ by $n_u$, $n_x$, $n_y$ and $n_p$ respectively. The matrix dimensions are then $A \in \mathbb{R}^{n_x \times n_x}$, $B \in \mathbb{R}^{n_x \times n_u}$, $C \in \mathbb{R}^{n_y \times n_x}$, $D \in \mathbb{R}^{n_y \times n_u}$. To impose some structure in the general LPV identification problem, we adopt an affine state space model, where the state space matrix coefficients depend linearly on the scheduling parameters $p_{(t)}$. The time-varying system matrices are then given by

$$A\big(p_{(t)}\big) = \sum_{i=1}^{n_p} A_i \, p_{i(t)} \tag{3}$$

where the matrices $A_i$ are constant. All the time-variance is due to the scheduling parameters $p_{i(t)}$. Identical definitions hold for $B\big(p_{(t)}\big)$, $C\big(p_{(t)}\big)$ and $D\big(p_{(t)}\big)$. Usually, $p_{1(t)} = 1$ to include the time-invariant case. In theory, $p_{(t)}$ can be any function of time. However, in line with Felici et al. [2007], we will use a dedicated periodic scheduling sequence for our identification experiment.

## 2. TIME DOMAIN STATE SPACE IDENTIFICATION

This section explains the basic ideas behind the subspace identification scheme. For the full details, we refer to Felici

et al. [2007]. By briefly reviewing the method to calculate the states and by extension the matrix coefficients, we can better highlight the differences between both approaches. The main goal is to estimate an observability matrix, as in the original LTI subspace algorithms Verhaegen and Yu [1995], Van Overschee and De Moor [1996], McKelvey et al. [1996]. From there, the $A_{(t)}$ and $C_{(t)}$ matrices can be estimated, and subsequently the $B_{(t)}$ and $D_{(t)}$ matrices.

### 2.1 Estimating the time-varying observability matrix

Starting from time step $t$, the $d$ successive outputs $y_t^d$ can be written as a function of the single initial state $x_t$ and the corresponding inputs $u_t^d$. To this end, first define the vertically stacked output vector $y_t^d$ as

$$y_t^d = \left[{y_{(t)}}^T,\, {y_{(t+1)}}^T,\, \ldots,\, {y_{(t+d-1)}}^T\right]^T \in \mathbb{R}^{(d\,n_y)\times 1}$$

and likewise the input $u_t^d$. Here $d$ is referred to as the time window size, which should be chosen somewhere between the order $n_x$ of the system and the period $P$ of the time variation: $P \geq d > n_x$. Then define the observability matrix $\mathcal{O}_t^d$

$$\mathcal{O}_t^d = \begin{bmatrix} C_{(t)} \\ C_{(t+1)}A_{(t)} \\ \vdots \\ C_{(t+d-1)}A_{(t+d-1)}\ldots A_{(t)} \end{bmatrix} \in \mathbb{R}^{(d\,n_y)\times n_x} \tag{4}$$

Next, take the input-to-output matrix $\mathcal{T}_t^d$ as in (5), at the bottom of the page. In the LTI case, $\mathcal{T}_t^d$ reduces to a block Toeplitz matrix. For all discrete time steps $t$ it holds that

$$y_t^d = \mathcal{O}_t^d x_{(t)} + \mathcal{T}_t^d u_t^d \tag{6}$$

Many rotating mechanical systems, like rotor-bearing systems Matthews [2009], have periodically time-varying dynamics. In the parameter-varying framework, we can impose periodicity by applying a recurring scheduling signal. The matrices $A_{(t)}$, $B_{(t)}$, $C_{(t)}$ and $D_{(t)}$ will then repeat after $P$ discrete time samples $A_{(t+P)} = A_{(t)}$. By extension, $\mathcal{O}$ and $\mathcal{T}$ then become periodic as well.

Finally, we can collect the data matrices over the periods

$$Y_t^d = \begin{bmatrix} y_t^d & y_{t+P}^d \cdots & y_{t+(N_P-3)P}^d \end{bmatrix} \in \mathbb{R}^{(d\,n_y)\times(N_P-2)} \tag{7}$$

and similarly $U_t^d$. Also

$$X_t = \begin{bmatrix} x_{(t)} & x_{(t+P)} \ldots & x_{(t+(N_P-3)P)} \end{bmatrix} \in \mathbb{R}^{n_x\times(N_P-2)} \tag{8}$$

Because of the periodicity, the data equation (6) can be extended $\forall\, t = 0 \ldots P-1$

$$Y_t^d = \mathcal{O}_t^d X_t + \mathcal{T}_t^d U_t \tag{9}$$

From the data equation (9) the column space of all the observability matrices $\mathcal{O}_t^d$ can be estimated, using only algebraic operators, like RQ factorization and SVD. The basic method only requires the input and output data $U_{t+P}^d$ and $Y_{t+P}^d$. By taking the $d$ past inputs and outputs $U_{t+P-d}^d$ and $Y_{t+P-d}^d$ as instrumental variables, unbiased estimates of $\mathcal{O}_t^d$ can be obtained even in the presence of white process and white output noise.

### 2.2 Coping with similarity transformations

The estimates $\hat{\mathcal{O}}_t^d$ are only determined up to a similarity transformation $T_{(t)}$, which will be different at each discrete time step $t$. It can easily be verified that the output $y_{(t)}$ remains exactly the same if we take a nonsingular matrix $T_{(t)}$ and define $x'_{(t)} = T_{(t)}\, x_{(t)}$, and also

$$\left[\begin{array}{c|c} A'_{(t)} & B'_{(t)} \\ \hline C'_{(t)} & D'_{(t)} \end{array}\right] \Leftrightarrow \left[\begin{array}{c|c} T_{(t+1)}A_{(t)}{T_{(t)}}^{-1} & T_{(t+1)}B_{(t)} \\ \hline C_{(t)}{T_{(t)}}^{-1} & D_{(t)} \end{array}\right] \tag{10}$$

The undetermined $T_{(t)}$ can be interpreted as each of the states $x_{(0)}$, $x_{(1)}$, …, $x_{(P-1)}$ being in a different state basis. Once all the $\hat{\mathcal{O}}_t^d$ are estimated $\forall\, 0 \leq t \leq P-1$, using the affine definition from equation (3), the calculated observability matrix $\hat{\mathcal{O}}_t^d$ can be written as a product between a time-varying weight matrix $M_t$ using only scheduling values, and a constant matrix $S$ that only depends on $A_i$ and $C_i$.

$$\hat{\mathcal{O}}_t^d T = \mathcal{O}_t^d = M_{t(p(t))} S_{(A_i,C_i)} \tag{11}$$

The matrix $M_t \in \mathbb{R}^{d\,n_y\times q}$ contains all the time-variation of $\mathcal{O}_t^d$, but its dimension $q = \sum_{j=1}^{d} n_y n_p^j$ explodes rapidly with the window size $d$. By solving (11) for all the factorized $\hat{\mathcal{O}}_t^d$ at the same time, the matrices are forced to use the same state basis.

$$\hat{\boldsymbol{\mathcal{O}}} T = \boldsymbol{M} S \tag{12}$$

$$T^T \hat{\boldsymbol{\mathcal{O}}}^T\, \hat{\boldsymbol{\mathcal{O}}} T = I_{n_x}, \qquad S^T \boldsymbol{M}^T\, \boldsymbol{M} S = I_{n_x} \tag{13}$$

$$\hat{\boldsymbol{\mathcal{O}}} = \text{blockdiag}\begin{pmatrix} \hat{\mathcal{O}}_0^d \\ \hat{\mathcal{O}}_1^d \\ \vdots \\ \hat{\mathcal{O}}_{P-1}^d \end{pmatrix}, \quad \boldsymbol{M} = \begin{bmatrix} M_0 \\ M_1 \\ \vdots \\ M_{P-1} \end{bmatrix} \tag{14}$$

with $\hat{\boldsymbol{\mathcal{O}}} \in \mathbb{R}^{(P d\, n_y)\times(P n_x)}$, $T \in \mathbb{R}^{(P n_x)\times n_x}$ and $\boldsymbol{M} \in \mathbb{R}^{(P d\, n_y)\times q}$. $\boldsymbol{M}$ is calculated and $\hat{\boldsymbol{\mathcal{O}}}$ is estimated. Alternatively, instead of working in the high-dimensional column space of $\boldsymbol{M}$, it is proposed to use the column space $\boldsymbol{M}\boldsymbol{M}^T$. This is beneficial when $q \gg P.d.n_y$.

To cope with process and output noise, the equality (12) can be replaced by minimizing the Frobenius norm of the difference between the left and right hand sides $\min_{T,S} \|\hat{\boldsymbol{\mathcal{O}}} T - \boldsymbol{M} S\|_F$. The problem is then restated as a canonical correlation analysis problem. To decrease the variance of the solution, at the cost of a bias, it is suggested to use a regularization constant $\nu$. The actual choice of the periodic scheduling sequence $p_{(t)}$ has an important effect on the degree of regularization required. In practice, $\nu$ will have to be gridded. In one of the examples in Felici et al. [2007], $\nu$ was scanned somewhere between $10^{-8}$ and $10^{4}$.

### 2.3 Obtaining the constant system matrices

Since the states are now in the same basis for all discrete time steps $t$, the $C_t$ and $A_t$ matrices can then be peeled from the observability matrices $\mathcal{O}_t^d$. Finally, the

$$\mathcal{T}_t^d = \begin{bmatrix} D_{(t)} & 0 & \ldots & 0 \\ C_{(t+1)}B_{(t)} & D_{(t+1)} & \ldots & 0 \\ C_{(t+2)}A_{(t+1)}B_{(t)} & C_{(t+2)}B_{(t+1)} & \ldots & 0 \\ \vdots & \vdots & \ddots & \vdots \\ C_{(t+d-1)}A_{(t+d-2)}\ldots A_{(t+1)}B_{(t)} & C_{(t+d-1)}A_{(t+d-2)}\ldots A_{(t+2)}B_{(t+1)} & \ldots & D_{(t+d-1)} \end{bmatrix} \tag{5}$$

remaining $B_{(t)}$ and $D_{(t)}$ are identified using simple least squares. From the local $A_{(t)}$, the constant matrices $A_i$ for $i = 1 \dots n_p$ can be calculated via (3). Exactly the same conversion is be used for $B_i$, $C_i$ and $D_i$.

## 3. FREQUENCY DOMAIN STATE SPACE IDENTIFICATION

The second global LPPV identification method performs the estimates in the frequency domain. It is shown that the transformed state space equations have a very specific structure when the input and scheduling are both periodic and synchronized. Even more, when the bandwidth of the scheduling sequence $p_{(t)}$ is limited, the SS representation becomes very sparse. In this section, the proposed algorithm is discussed step by step. Section 4 elaborates on the advantages and disadvantages of the frequency and time domain approaches.

### *3.1 From time to frequency domain*

If a periodic input and periodic scheduling is applied, and an integer number of periods of both signals is measured (synchronized acquisition), the state space equations (1)-(2) can be transformed from the time domain to the frequency domain without leakage errors. The Z-transform is used for the formulas (1)-(2) and the Discrete Fourier Transform (DFT) is applied to the measurements $u_{(t)}$ and $y_{(t)}$. The multiplication of two time signals is equivalent to the convolution $*$ of their spectra. Since we are working in a discrete periodic framework, this convolution is circular.

$$zX(z) = A_{(z)} * X_{(z)} + B_{(z)} * U_{(z)} \tag{15}$$
$$Y(z) = C_{(z)} * X_{(z)} + D_{(z)} * U_{(z)} \tag{16}$$

As in the affine definition (3) in the time domain, the dynamics and the time variation can be separated in the frequency domain. We find a multiplication of the dynamics $A_i$, $B_i$, $C_i$ and $D_i$ and their associated scheduling spectra $\mu_{i(z)}$ for each discrete frequency $z = e^{j2\pi k/N}$.

$$A_{(z)} = \sum_{i=1}^{n_p} A_i \, \mu_{i(z)} \tag{17}$$

Note that the constant matrices $A_i$ are identical in the time domain (3) and the frequency domain (17) notation. If we collect the equations for all $k$, we get

$$E.X = \alpha \, \mu_x X + \beta \, \mu_u U \tag{18}$$
$$Y = \gamma \, \mu_x X + \delta \, \mu_u U \tag{19}$$

where $U \in \mathbb{C}^{(n_u N)\times 1}$, $X \in \mathbb{C}^{(n_x N)\times 1}$ and $Y \in \mathbb{C}^{(n_y N)\times 1}$ are vectors containing the stacked spectra of the state, input and output for all discrete frequencies $k$, and

$$E = I_{n_x} \otimes \operatorname{diag}\left(1, e^{j2\pi\frac{1}{N}}, \dots, e^{j2\pi\frac{N-1}{N}}\right) \tag{20}$$

$$\mu_x = \begin{bmatrix} \operatorname{Toeplitz}\left(\mu_1, \mu_1^H\right) \otimes I_{n_x} \\ \vdots \\ \operatorname{Toeplitz}\left(\mu_{n_p}, \mu_{n_p}^H\right) \otimes I_{n_x} \end{bmatrix} \tag{21}$$

$$\mu_u = \begin{bmatrix} \operatorname{Toeplitz}\left(\mu_1, \mu_1^H\right) \otimes I_{n_u} \\ \vdots \\ \operatorname{Toeplitz}\left(\mu_{n_p}, \mu_{n_p}^H\right) \otimes I_{n_u} \end{bmatrix} \tag{22}$$

$$\alpha = \left[A_1 \otimes I_N \middle| A_2 \otimes I_N \middle| \dots \middle| A_{n_p} \otimes I_N\right] \tag{23}$$
$$\beta = \left[B_1 \otimes I_N \middle| B_2 \otimes I_N \middle| \dots \middle| B_{n_p} \otimes I_N\right] \tag{24}$$
$$\gamma = \left[C_1 \otimes I_N \middle| C_2 \otimes I_N \middle| \dots \middle| C_{n_p} \otimes I_N\right] \tag{25}$$
$$\delta = \left[D_1 \otimes I_N \middle| D_2 \otimes I_N \middle| \dots \middle| D_{n_p} \otimes I_N\right] \tag{26}$$

The cyclic convolution has been rewriten as a matrix product using the block Toeplitz matrices $\mu_x$ and $\mu_u$.

In the LTI framework, the responses at different frequencies are decoupled. This is no longer the case for an LPV system: the output equations are coupled over the frequencies and, therefore, have to be computed for all frequencies at once.

If the scheduling has only a limited bandwidth, the resulting SS representation becomes very sparse, as illustrated in Figure 1 for a 2nd order SISO LPV system. Because of this sparsity, the output can be computed time-efficiently. Since the output has to be evaluated at each iteration of the optimization algorithm, for all $(n_x + n_y)n_p(n_x + n_u)$ parameters, this is an important result.

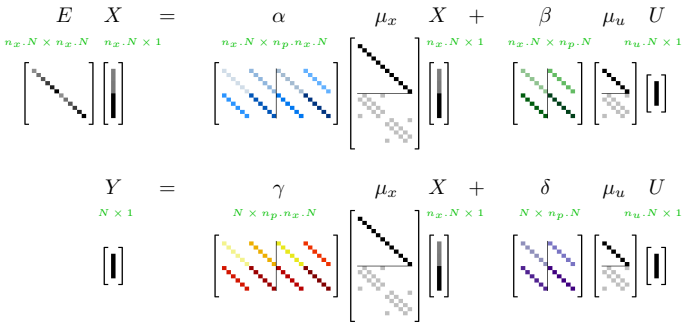


Figure 1. State Space equations in the frequency domain for a 2nd order Single Input Single Output (SISO) LPV system, collected for all frequencies. The periodic scheduling results in a structured representation.

### *3.2 Optimization*

In line with Lee and Poolla [1999], a non-linear optimization routine is used to calculate the unknown constant matrices $A_i$, $B_i$, $C_i$ and $D_i$. In the case of an Output Error (OE) stochastic framework, it is possible to calculate the Jacobian analytically. Since the state space representation is sparse in the frequency domain, it can be calculated time-efficiently as well. Future research will focus on extending our approach to input noise.

For a given model with parameters $\theta$, the (complex) output error is defined as $e(\theta) = Y_{\text{model}} - Y_{\text{measured}}$. The Maximum Likelihood Estimator (MLE) then finds the parameters $\hat{\theta}_{\text{ML}}$ that minimize the non-linear least squares cost function $V_{\text{ML}}$:

$$\begin{aligned}\hat{\theta}_{\text{ML}} &= \underset{\theta}{\operatorname{argmin}} \, V_{\text{ML}}(\theta, Z) \\ &= \underset{\theta}{\operatorname{argmin}} \, e(\theta)^H C_e^{-1}{}_{(\theta)} e(\theta)\end{aligned} \tag{27}$$

where $C_{e(\theta)} = \operatorname{cov}\left(e(\theta)\right)$ is the covariance matrix. If only output noise is present, it is parameter-independent.

A great advantage of working with synchronized data is that we can estimate the noise covariance matrix $C_e$ in a pre-processing step prior to the parametric modeling

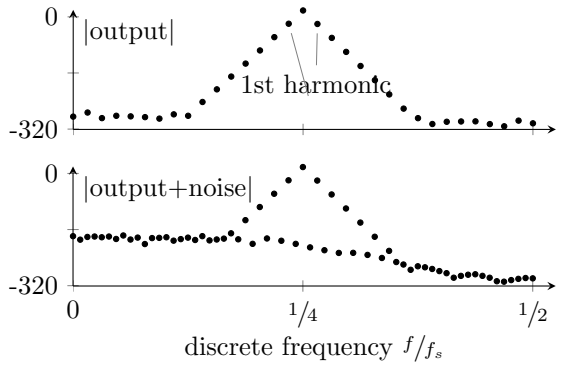


Figure 2. Output spectrum (in dB) of an LPV system when a single sine is applied to the input. Measuring extra periods allows for an estimate of the noise covariance matrix $C_e$. Because we only excite certain frequencies, energy on spectral lines in between can only originate from the noise.

of the time-invariant plants dynamics. The basic idea is explained at the end of this subsection. Let us first take a look at the frequency response of an LPPV system to a single sine wave, depicted in the top of Figure 2. Only the center frequency $f_u = {}^{f_s}/_4$ was exited. As in Lataire and Pintelon [2011], the time variation then results in responses at neighboring frequencies in the shape of a skirt. However, these skirts can only appear at what we call harmonic frequencies : $f_u + kf_p$. Here, $f_p$ is the frequency of the periodic parameter variation and $k \in \mathbb{Z}$. Since our input and scheduling signals are periodic, measuring multiple periods causes gaps in between the excited harmonics. The spectral resolution will improve, meaning there will be more frequency lines. The same input frequency $f_u$ is excited, and the LPPV system can only influence the harmonic frequencies. Thus if there is energy at the extra intermediate spectral lines, it must originate from a (possibly colored) noise source, as is illustrated by the lower graph in Figure 2. We can therefore estimate a non-parametric noise model $\hat{C}_e$ from the gaps in between the harmonics.

### *3.3 Initial model estimate*

It is widely known that a good initial estimate is of paramount importance in non-linear optimization. We opt for the Best Linear Time-Invariant (BLTI) approximation defined in Lataire et al. [2012], Pintelon et al. [2012]. Basically, an LTI model is estimated using the input frequencies $f_u$ and the first harmonics $f_u \pm f_p$. This results in an estimate of the time-invariant $A_1$ and $C_1$, but for every $B_i$ and $D_i$. A similar approach is proposed in Lee and Poolla [1999]. In Casella and Lovera [2008], this is called an input-affine LPV model. In fact, the input $u_{(t)}$ is extended by multiplication with each component of the scheduling $p_{(t)}$. Equations (28)-(29) illustrate the identifiable blocks for a system with one varying scheduling parameter. Recall that $p_{1(t)} = 1$, thus $\mu_1$ equals the identity matrix $I_{n_x} \otimes I_N$.

$$EX = [\alpha_1|\cancel{\alpha_2}] \begin{bmatrix} \mu_1 \\ \mu_2 \end{bmatrix} X + [\beta_1|\beta_2] \begin{bmatrix} \mu_1 \\ \mu_2 \end{bmatrix} U \tag{28}$$

$$Y = [\gamma_1|\cancel{\gamma_2}] \begin{bmatrix} \mu_1 \\ \mu_2 \end{bmatrix} X + [\delta_1|\delta_2] \begin{bmatrix} \mu_1 \\ \mu_2 \end{bmatrix} U \tag{29}$$

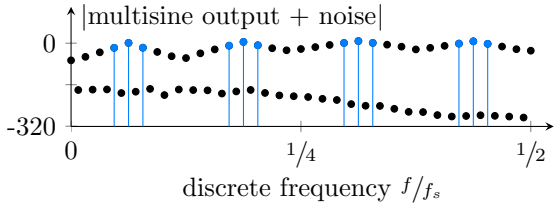


Figure 3. Frequency response (in dB) of an LPV system to a multisine input. If the difference between the excited frequencies is large enough, the skirts overlap less. The initial LTI model with extended inputs uses the excited frequencies $f_u$ and the first harmonics $f_u \pm f_p$.

$\alpha_1$, $\beta_1$, $\gamma_1$ and $\delta_1$ define an LTI system. By taking a new, extended input $U' = \mu_u U$ with $\mu_u$ defined in (22), the first harmonics are excited, and $\beta_2$ and $\delta_2$ can be estimated with an LTI model. This BLTI approximation with extended inputs can be improved by an appropriate design of the multisine input. As illustrated in Figure 3, if the spacing in between the input frequencies $f_u$ is large enough, the ever-fading skirts will overlap less, and a better LTI estimate can be obtained. In all our experiments, this initialization has appeared to be "close enough" to the global optimum. The trade-off lies in the spectral resolution of the frequency response and the accuracy of the parameter-varying dynamics. A denser multisine makes the skirt overlap more, causing the BLTI approximation to become less accurate. If the optimization does not get stuck in a local minimum, the final estimated model should yield a better fit of the dynamics.

## 4. DISCUSSION AND COMPARISON

### *4.1 Time domain*

The time domain approach is based on solid linear algebra. However, there are some parameters to be chosen. In the periodic-MOESP method, the problem size is reduced because of the smaller window size $d < P$, compared with the lifting procedure in Hench [1995], which uses the full period $P$. Although it seems logical to take $d = P$, based on experience, it is reported that less accurate results are obtained when the window length $d$ grows much larger than the state dimension $n_x$. Finally, the regularization parameter $\nu$ has to be chosen. It weights a reduction of the variance of the solutions versus a bias. The bigger $\nu$ becomes, the less accurate the overall fit will be. For a third order SIMO example, regularization is already necessary, otherwise the estimated model will be poor. In practice, $\nu$ will have to be gridded and tested on validation data for each identification experiment.

In the appendix of Felici et al. [2007], a proof is given that for $N \to \infty$, $\hat{\mathcal{O}}_t^d$ from (9) converges to the column space of the observability matrix $\mathcal{O}_t^d$. However, because of the unknown influence of the window $d$ and the regularization constant $\nu$ on the resulting fit, it is hard to predict the total error on the estimated model.
A big advantage of the periodic-MOESP is that is inherently designed to handle both output and process noise, while the frequency domain approach currently only takes the output noise into account. In future research, input noise will be added to the LPPV framework.

### 4.2 Frequency domain

The important difference with the time-domain periodic-MOESP method is that a multisine, a sum of random phase sine waves, is applied at the input. So both the scheduling and the input are periodic. Although the demand of periodic input and scheduling will rule out some applications, there are certain advantages over a random input. Measuring several periods results in a reduction of the noise level in the frequency domain. One can think of it as averaging out a mean where the accuracy increases with the square root of the number of periods O $\left(\sqrt{N_p}\right)$. In the limit $N_p \to \infty$, the Fourier coefficients will converge to the correct values, and the noise influence is eliminated. The variance due to the time variation cannot be captured by the BLTI model, it will remain the same for large $N_p$.

For $N_p \geq 2$ the output noise power spectrum can be estimated, as explained in Section 3.2. Colored output noise is therefore no problem. Another important asset is that we can get a smooth input spectrum at the frequency band of interest. Every extra period lowers the overall noise level. This allows for a better signal to noise ratio in the most important dynamics region, and will thus lead to a better estimation.

We want to stress that there are no identification parameters to be tuned once the experiment is designed. There is no curse of dimensionality, because the matrices grow linearly with the period $P$, the order $n_x$ of the system and the number of scheduling parameters $n_p$. Even so, because of the coupling over the frequency of the output equations, we do have to compute the output for all frequencies at once. However, since the compact notation (18)-(19) inherently incorporates the affine structure, we do not need to concern ourselves with the states being in different basis, like in (11).

## 5. SIMULATION EXAMPLE

We illustrate both identification methods on a Single Input, Single Output (SISO) LPV example: the flapping dynamics of a wind turbine from van Wingerden [2008]. The cosine of the blade rotation angle yields the periodic scheduling sequence. We have

$$[A^{(0)}|A^{(1)}] = \left[\begin{array}{cc|cc} 0 & 0.0734 & -.0021 & 0 \\ -6.5229 & -.4997 & -.0138 & .5196 \end{array}\right]$$

$$[B^{(0)}|B^{(1)}] = \left[\begin{array}{c|c} 0 & 0 \\ -9.6277 & 0 \end{array}\right]$$

$$[C^{(0)}|C^{(1)}] = \left[\begin{array}{cc|cc} 1 & 0 & 0 & 0 \end{array}\right]$$

$$[D^{(0)}|D^{(1)}] = \left[\begin{array}{c|c} 0 & 0 \end{array}\right]$$

As in Felici et al. [2007], 50 000 discrete time steps are taken. For the periodic-MOESP method, this system is excited using white noise. The frequency domain approach requires a synchronized, periodic input, and thus a random phase multisine is applied, with a period $P = 500$. The periodic scheduling is taken $p(t) = [1\,,\, \cos(2\pi \frac{1}{10} t)]$ A drawback of the current frequency domain approach is that the measurements must be performed in steady state, so the inputs, states and outputs are all periodic. We therefore have to wait until the transients have died out. In this case, the first measurement period is discarded, and

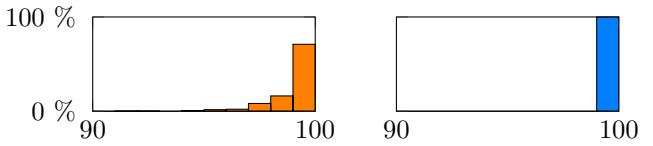


(a) time domain method (b) frequency domain method

Figure 4. Histogram of the Variance Accounted For, for both LPV identification techniques.

$N_p = 99$ periods remain. In future work we will extend the LPV framework to model this transient behavior as well.

The identified models are validated on an independent data set, where the input is a white random noise signal, with the mean $\mathbb{E}\{u_{\text{val}(t)}\} = 10$ and a standard deviation $\sigma\{u_{\text{val}(t)}\} = 1$. From a theoretical point of view, the identified model can be used for arbitrary and non-periodic scheduling and inputs. This is only true if the selected model structure is exact. For a practical application, we better do not extrapolate the dynamical behavior for a single parameter frequency to the full frequency band. Therefore, the validation scheduling is chosen to be a shifted version of the experimental setup : $p_{\text{val}(t)} = [1\,,\, \cos(2\pi \frac{1}{10} t + \phi)]$. As a measure of performance the Variance-Accounted-For (VAF) is used. It is defined as

$$\text{VAF} = \max\left\{1 - \frac{var\big(y_{(t)} - \hat{y}_{(t)}\big)}{var\big(y_{(t)}\big)}, 0\right\} \times 100 \qquad (30)$$

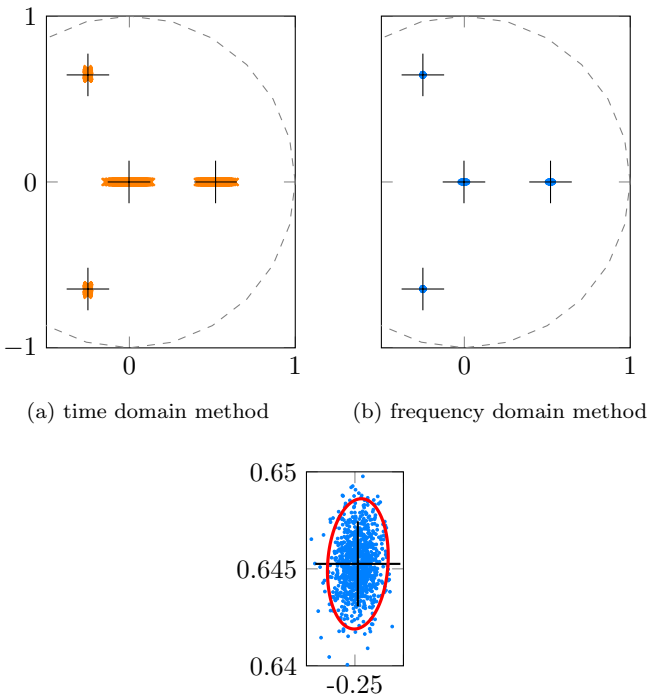


(a) time domain method (b) frequency domain method

(c) 95% confidence Cramér-Rao uncertainty ellipse of the frequency domain estimates. 6.7% of the estimated eigenvalues are outside of the 95% confidence bound.

Figure 5. Estimated invariant eigenvalues of the constant matrices $A_i$ in the complex plane. The big crosses (✚) indicate the poles of the underlying system. The orange crosses (×) on the left plot show the time domain estimates, while the blue dots (•) on the right correspond to the frequency domain method.

where $\hat{y}_{(t)}$ denotes the output signal obtained by simulating the identified LPV system, and with $y_{(t)}$ the noiseless output signal of the true system. Figures 4 and 5 show the results of 1000 Monte Carlo simulations with different noise realizations, but identical experimental conditions. Figure 4 displays a histogram of the VAF. The frequency domain approach consistently yields a better fit on the validation data. The mean VAF is 99.998 with a standard deviation of 0.0016. Although the periodic-MOESP does fairly well, there is more variability in its estimates.

Because of similarity transformations (10), each identified model can be in a different state basis. However, the eigenvalues of the $A_i$ matrices remain invariant. They can be interpreted as the poles of the harmonic transfer functions. The performance can therefore also be deduced from the pole plots depicted by Figure 5. Again, we see that there is much more variance in the periodic MOESP estimates. The results from the frequency domain approach seems to converge to the true values. In fact, we can calculate the Cramér-Rao lower bound on the variance of the eigenvalues, by extending the perturbation analysis in Golub and Van Loan [1996]. For the real poles, we can then construct a 95% confidence interval. For the complex conjugate poles, we find 95% confidence ellipses. Figure 5c illustrates how 93.7% of the frequency domain estimates fall within the Cramér-Rao uncertainty ellipse. The proposed new method is therefore not only consistent, but also asymptotically efficient!

## 6. CONCLUSION

Two state of the art global LPV state space identification schemes where discussed. The frequency domain method requires synchronized input and scheduling sequences, and may therefore not be applicable to every application. For the output error case, the proposed frequency domain method is consistent and asymptotically efficient even in the presence of colored output noise, while the periodic MOESP has higher variance and is restricted to white noise. Note however that the latter can also tackle (white) process noise, and works with arbitrary inputs. Future research will be dedicated to the extension of the frequency domain method, to eliminate these shortcomings.

## ACKNOWLEDGEMENTS

This work was supported in part by the Fund for Scientific Research (FWO-Vlaanderen), by the Flemish Government (Methusalem Fund, METH1), and by the Belgian Federal Government (IUAP VII, DYSCO).

## REFERENCES

F. Casella and M. Lovera. LPV/LFT modelling and identification: overview, synergies and a case study. In *IEEE International Symposium on Computer Aided Control System Design*, pages 852–857, 2008.

J. De Caigny. *Contributions to the Modeling and Control of Linear Parameter-Varying Systems'*. PhD thesis, K.U. Leuven, 2009.

F. Felici, J.W. van Wingerden, and M. Verhaegen. Subspace identification of MIMO LPV systems using a periodic scheduling sequence. *Automatica*, 43:1684–1697, 2007.

G. Golub and C. Van Loan. *Matrix Computations (3d ed.)*. The John Hopkins University Press, 1996.

J. J. Hench. A technique for the identification of linear periodic state-space models. *International Journal of Control*, 62(2):289–301, 1995.

J. Lataire and R. Pintelon. Frequency domain weighted nonlinear least squares estimation of continuous-time, time-varying systems. *IET Control Theory & Applications*, 5(7):923–933, 2011.

J. Lataire, E. Louarroudi, and R. Pintelon. Detecting a time-varying behavior in frequency response function measurements. *IEEE Trans. Instrum. and Meas.*, 61 (8):2132–2143, 2012.

L. H. Lee and K. Poolla. Identification of linear parameter-varying systems using nonlinear programming. *Proceedings of the 35th IEEE Conference on Decision and Control*, 121(1):71–78, 1999.

S.M. Lee and Ju H. Park. Output feedback model predictive control for LPV systems using parameter-dependent lyapunov function. *Applied Mathematics and Computation*, 190(1):671–676, 2007.

L. Ljung. *System Identification : Theory for the User*. Prentice Hall, Upper Saddle River, NJ, USA, 1999.

E. Louarroudi, J. Lataire, R. Pintelon, P. Janssens, and J. Swevers. Parametric estimation of the evolution of the time-varying dynamics of periodically time-varying systems from noisy input-output observations. *Mechanical Systems and Signal Processing*, 2012. doi: 10.1016/j.ymssp.2013.03.013i. accepted for publication.

A. Matthews. Frequency-domain identification of linear time-periodic systems using lti techniques. *Journal of Computational and Nonlinear Dynamics*, 4(4), 2009.

T. McKelvey, H. Akcay, and L. Ljung. Subspace-based multivariable system identification from frequency response data. *IEEE Transactions on Automatic Control*, 41(7):960–978, 1996.

D. Petersson and J. Löfberg. LPV H2-controller synthesis using nonlinear programming. In *Proceedings of the 18th IFAC World Congress*, pages 6692–6696, Milan, Italy, 2011. doi: 10.3182/20110828-6-IT-1002.02028.

R. Pintelon, E. Louarroudi, and J. Lataire. Detection and quantification of the influence of time variation in frequency response function measurements using arbitrary excitations. *IEEE Trans. Instrum. and Meas.*, 61(12): 3387–3395, 2012.

W. J. Rugh and J. S. Shamma. Research on gain scheduling. *Automatica*, 36(10):1401–1425, 2000.

R. Tóth. *Modeling and Identification of Linear Parameter-Varying Systems*. Springer Germany, 2010.

R. Tóth, H. S. Abbas, and H. Werner. On the state space realisation of LPV input-output models : practical approaches. *IEEE transactions on control systems technology*, 20(1):139–153, 2012.

P. Van Overschee and B. De Moor. *Subspace Identification for Linear Systems: Theory, Implementation, Applications*. Kluwer Academic Publishers, 1996.

J.W. van Wingerden. *Control of Wind Turbines with Smart Rotors*. PhD thesis, Technische Universiteit Delft, 2008.

M. Verhaegen and X. Yu. A class of subspace model identification algorithms to identify periodically and arbitrarily time-varying systems. *Automatica*, 31(2): 201–216, 1995.